FOCUSED ULTRASOUND TRANSDUCER WITH ELECTRICALLY CONTROLLABLE FOCAL LENGTH

Lurui Zhao and Eun Sok Kim
Department of Electrical Engineering-Electrophysics
University of Southern California, Los Angeles, CA 90089-0271, U.S.A.

ABSTRACT

This paper reports a novel acoustic transducer capable of delivering focused acoustic beam with electrically tunable focal length over 7 mm. Constructed on a 1.02 mm thick lead zirconate titanate (PZT) substrate, the transducer uses a collection of equal-width-equal-spacing concentric ring electrodes (and a circular electrode at the center) on one side of the substrate. With each electrode individually addressable, a desired focal length is mapped to a set of the electrodes generating the acoustic waves that arrive at the focal point in-phase for constructive interference. We have demonstrated a device capable of electrically tuning the focal length (of a focal spot of sub-mm in diameter) from 5 to 12 mm, with the electrical tunability confirmed through droplet ejection from liquid surface (that is at the focal plane), as the liquid level is varied.

INTRODUCTION

Focused ultrasound (FUS) has a wide application potential in imaging [1], tumor treatment [2], neuron stimulation [3], etc. However, all the previously designed transducers [4-6] are of a fixed focal length, with no electrical controllability for the focal length, and are incapable of dynamically changing the focal spot without physically moving the transducer. The new device described here offers tremendous degree of operating freedom by enabling the electrical controllability of the focal length. By using the new design, a real-time, fast-response, on-demand changing of focal length can be achieved.

DESIGN

The transducer is built on a 1.02 mm thick PZT substrate, whose fundamental thickness-mode resonant frequency is 2.25 MHz. Two layers of nickel sputtered on both sides which serve as electrodes. Ultrasonic waves are generated at the areas covered by patterned nickel electrodes due to the PZT's piezoelectric effect. The electrode patterns are designed to have one (1) circular center and thirty-one (31) concentric equal-width annular rings (outside the center electrode), for a total of 32 electrodes. Each and every one of the 32 patterned electrodes is wired out to a pad with individual accessibility. The radius of the circular center electrode is 2 mm, while the width of each of the annular ring is 0.2 mm with equal spacing of 0.05 mm between two adjacent electrodes.

Electrical controlling the focal length is achieved by selecting a group of electrodes to actuate so that the acoustic waves generated from those selected electrodes will arrive at the desired focal length in-phase, interfere constructively, and create a focal spot of high acoustic intensity. As each electrode can be selected or unselected, the 32 electrodes give a 32-bit resolution of controlling precision. Figure 1 illustrates a 4-bit transducer. Higher bit resolution will give more precise control over the focal length.

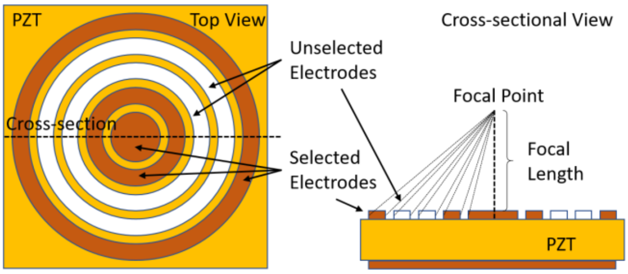

Figure 1: Top-view and cross-sectional view schematics of a 4-bit resolution transducer. Four equal-width concentric ring electrodes are patterned on PZT. Each electrode can be actuated individually. By varying the selection of the electrodes to be actuated, the focal length can be varied.

The radius of the circular center electrode r_0 approximately defines the lower bound of focal length, as suggest by:

$$f_{min} = \frac{\sqrt{r_0^2 + \lambda^2/4}}{\lambda} \quad (1)$$

For the n^th ring electrode, we use its central radius (average of inner and outer radius) to calculate the contribution to the focal point according to their phase factor (P.F.):

$$P.F. = \sin\left(\frac{\sqrt{r_n^2 + f^2} - f}{\lambda} \cdot 2\pi\right) \quad (2)$$

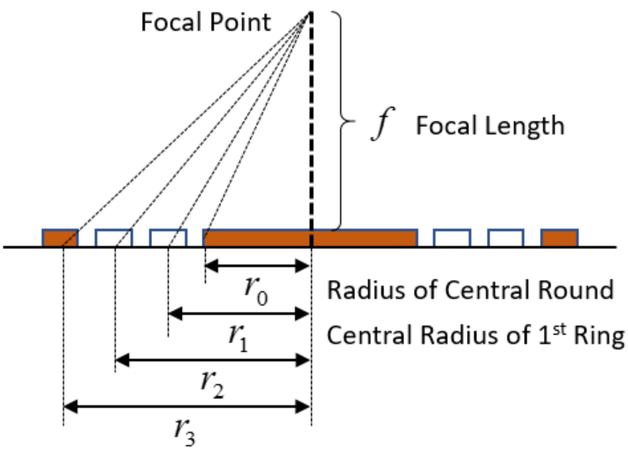

Figure 2: The radius of the circular center electrode r_0 determines lower bound of the focal length approximately. The n^{th} radius r_n is used to determine if the n^{th} ring electrode needs to be actuated of a particular focal length.

If the contribution is positive for in-phase constructive interference, we will add this electrode into the group of the electrodes to be actuated. Otherwise (i.e., out-of-phase destructive interference), we will not select the ring to actuate. Figure 3 demonstrates the actuation selection group based on our 32-bit transducer design. As we vary the focal length, the actual focal size will change accordingly: a shorter focal length will result in a smaller focal size, while a longer focal length will induce a larger focal size.

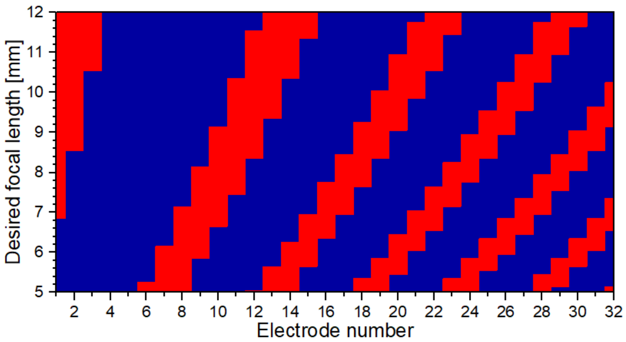

Figure 3: A plan for selecting the actuation group of the electrodes for a 32-bit resolution transducer. The red blocks mean the corresponding n^{th} electrode rings are selected for actuation, while the blue ones means unselected.

SIMULATION

Simulation on particle displacement (that is directly related to acoustic intensity) is carried out to verify the initial design as well as the capability to control the focal length. A C++ FEM program has been coded based on the piezoelectricity and acoustics, and data visualization has been achieved by another Python program. To make a clear demonstration of the electrical controllability of the focal length, we choose 4 typical focal lengths (5, 7, 10, and 12 mm) to run the simulation. For the four cases, we simulate on the same electrode patterning (32-bit) but different sets of the actuated electrodes from Figure 3.

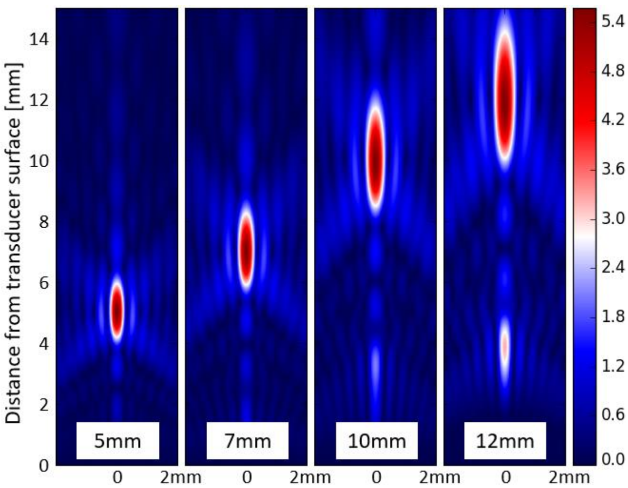

Figure 4: Simulation results showing the focal effect and focal length of 5, 7, 10 and 12 mm.

The simulated results on the vertical cross-sectional particle displacement are shown in Figure 4 for each of the four focal-length actuating selections. Focal effects are significant with an elliptical focal region at the desired focal length. The particle displacement at the focal spot is about 10 times larger than the average value of the particle displacements in the rest of the region. As expected, the focal size is dependent on the focal length.

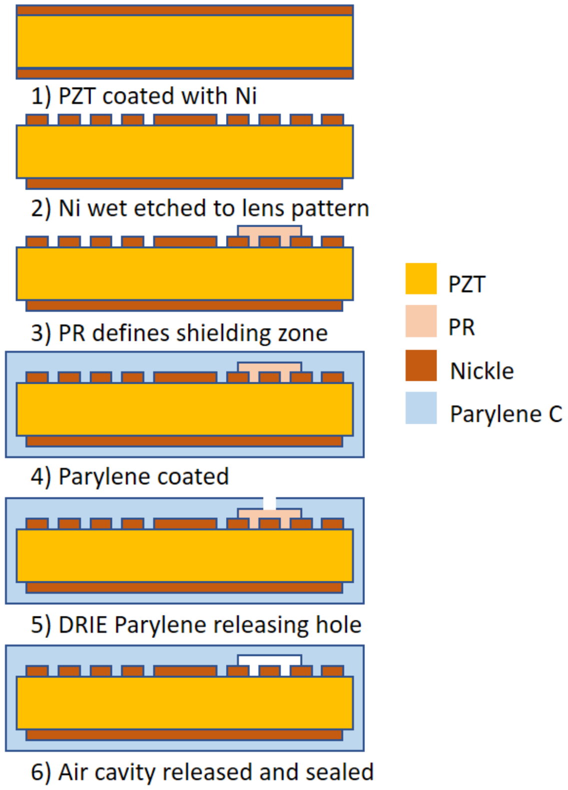

Figure 5: Fabrication process of the transducer.

FABRICATION

A brief fabrication process is illustrated in Figure 5. We start with a 1.03mm thick PSI-5A4E PZT sheet with nickel layer sputter-deposited on its both sides. AZ5214 photoresist is coated for both front and back sides for the electrode pattern delineation. Front-to-back alignment is done by aligning at the pre-defined dicing edge of PZT sheet. The electrode wiring-outs are patterned on the front side. After the wet etch of nickel layer, a second layer of photoresist is spin-coated for a sacrifice layer in forming air cavities which block acoustic waves in the region (and its conjugate region) where annular rings are disturbed for electrical wiring-outs (so that the acoustic-wave sources may be circumferentially symmetric). Then, with the protection of the backside electrode, a 6μm thick Parylene film is deposited, and release holes are defined on the front side where air cavities are needed. Oxygen reactive ion etch (RIE) is used to etch through the Parylene to form the release holes, and the sacrificial layer is removed by acetone through the release holes. A second layer of Parylene film is, then, deposited to seal the holes to finish the air-cavity reflectors and provide the transducer with electrical insulation for liquid immersive operations. The finished transducer is shown in Figure 6.

Different packages may be used for different applications. We build an acrylic handler to house the transducer and position it under water for verifying the focal length through droplet ejection experiment. Reservoir based package is also adopted for other application and operation.

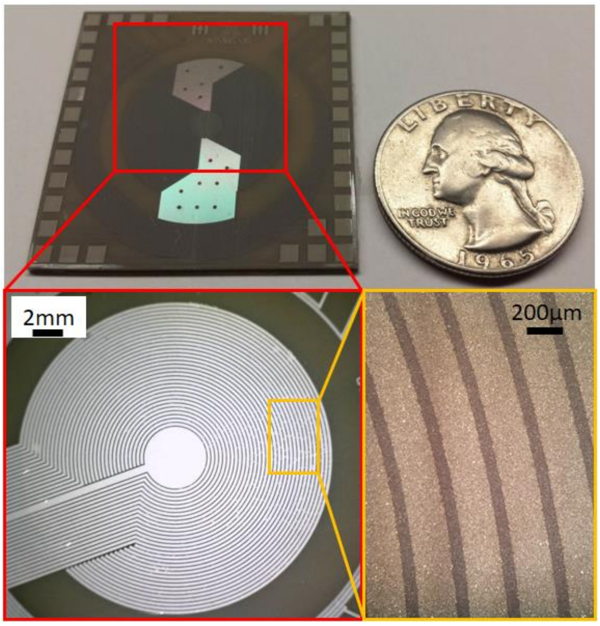

Figure 6: Photos of the fabricated transducer. The top photo shows the transducer after releasing sacrificial photoresist layer for air reflector region which shelters the asymmetric electrode part. The O_2 plasma etched releasing hole can be clearly seen. The bottom photos show the close-up views of the patterned electrodes.

MEASUREMENT

We use water-droplet ejection to verify the focal length, focal size and electrical-focal-length controllability. When the liquid level is right at the focal plane, the water within the focal spot will receive an intensified acoustic energy from the focused ultrasound, which leads to ejection of water droplets. By observing the droplet ejection, we can measure the focal length from the water height at which the droplet ejection occurs (as the focused ultrasound is the one that causes the ejection) and the lateral focal size (which is closely related to the droplet size).

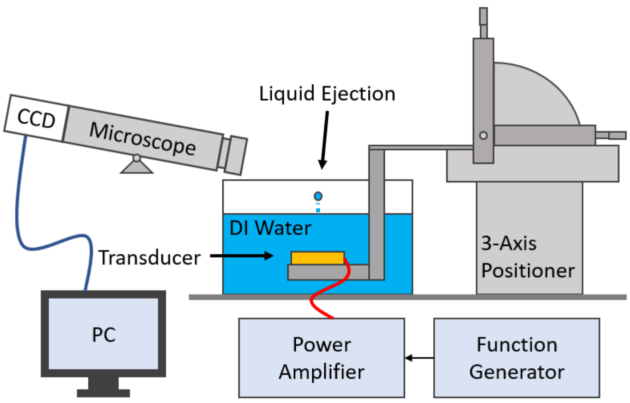

Figure 7: Measurement setup schematics for droplet ejection experiment. Droplet ejection can be observed by CCD camera, while the focal length can be measured with the micropositioner.

Figure 7 illustrates the measurement setup schematics for our transducer. The function generator outputs the driving waveform of pulsed sinusoidal wave of 2.25 MHz, 200 pulse cycles at a pulse repetition frequency of 60 Hz, which then is amplified to around 430 V_{pp} by a power amplifier. A 3-axis positioner holds the acrylic handler to position the transducer within the water. A CCD camera is attached to a long-range microscope for observing the droplet ejection from the side, with a synchronized delay-adjustable light strobing with light-emitting-diode (LED) working as a stroboscope for capturing the ejection process at various points in time.

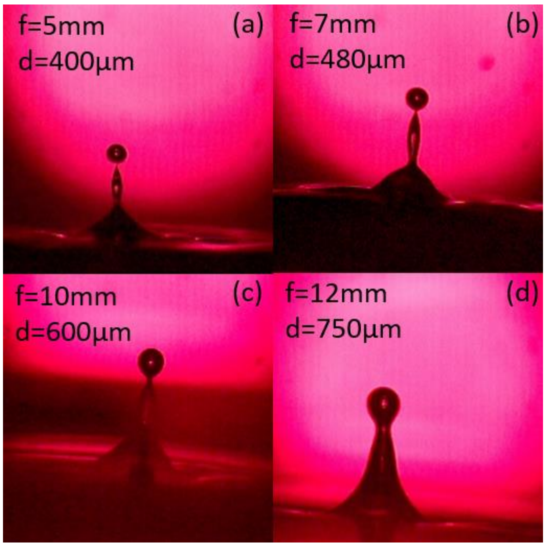

Figure 8: Cross-sectional-view photos of the water ejections obtained at the water heights of 5 mm (a), 7 mm (b), 10 mm (c), and 12 mm (d).

RESULTS

When our transducer is positioned at the desired focal length under the water surface, the droplet ejection occurs, and the water height is recorded as the transducer's focal length. By changing the delay from the stroboscopic LED to the moment when the droplet ejection starts (after necking of a water column), we measure the lateral size of the droplet.

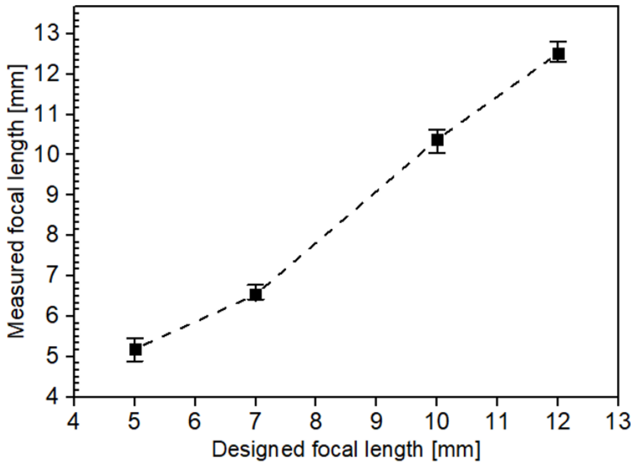

Figure 9: Measured focal lengths vs designed focal lengths.

Each of the photos in Figure 8 shows the necking of the water column just before a droplet is ejected. The diameter of the droplet is measured from the captured video. The water height is read out from the positioner. The graph in Figure 9 shows the relation between the designed focal length (by the actuation plan) versus the measured focal length. The graph in Figure 10 summarizes the measured lateral dimensions of the droplets in Figure 8 with respect to the set focal lengths, as well as the simulated focal sizes from our C++ program.

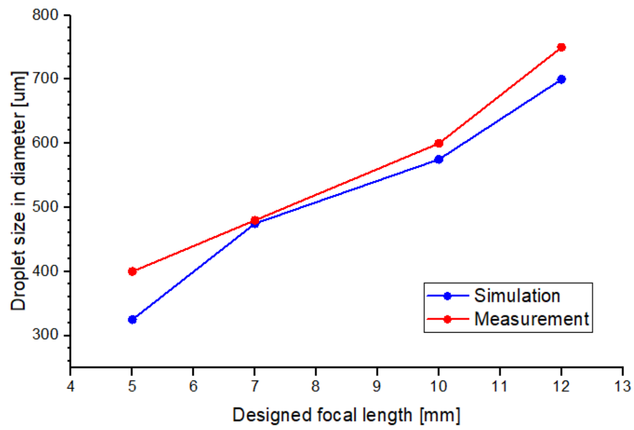

Figure 10: Ejected droplet size vs designed focal length (both measured and simulated data).

CONCLUSION

We have designed and fabricated a 32-bit focus ultrasonic transducer with electrically controllable focal length from 5 to 12 mm, with a controllable range of 7 mm. Simulations carried out with a C++/Python program show the cross-sectional views of four typical focal-lengths (5, 7, 10, and 12 mm), showing that the focal length can be varied via electrical selection of a proper set of the electrodes.

The transducer is tested through liquid droplet ejections to demonstrate the tunability of the focal length. When the transducer is configured for a particular focal length, we measure to focal length by finding the water level where the ejection occurs, as we vary the water height. Under various actuating conditions, the focal lengths are measured, and compared to the designed focal lengths. The size of the ejected liquid droplet (corresponding to the focal size) is measured (and simulated) to vary between 400 and 800 μm in diameter, and be dependent on the focal length.

ACKNOWLEDGEMENTS

This paper is based on the work supported by National Institutes of Health under grant R21EB022932.

REFERENCES

[1] S. Vaezy, et al, "Real-time visualization of high-intensity focused ultrasound treatment using ultrasound imaging", *Ultrasound in Medicine & Biology, Volume 27, Issue 1, January 2001, Pages 33-42*

[2] E. A. Stewart, et al, "Focused ultrasound treatment of uterine fibroid tumors: Safety and feasibility of a noninvasive thermoablative technique", *American Journal of Obstetrics and Gynecology, Volume 189, Issue 1, July 2003, Pages 48-54*

[3] M. D. Menz, et al, "Precise Neural Stimulation in the Retina Using Focused Ultrasound", *Journal of Neuroscience 6 March 2013, 33 (10) 4550-4560*

[4] D. Huang, E. S. Kim, "Micromachined Acoustic-Wave Liquid Ejector", *Journal of Microelectromechanical Systems, vol. 10, no. 3, pp. 442-449, 2001.*

[5] C. Lee, H. Yu, E. S. Kim, "Acoustic Ejector with Novel Lens Employing Air-Reflectors", *in IEEE International Micro Electro Mechanical Systems Conference, Istanbul, Turkey, January 22-26, 2006, pp. 170-173.*

[6] L. Wang, C.-P. Liao, M. Gross, and E.S. Kim, "Self-Focusing Acoustic Transducer (SFAT) with 10 mm Focal Length for Cancer-Specific Localized Cytolysis of 3D Cell Spheroids in 3D Matrigel," *Transducers '13, The 17th International Conference on Solid-State Sensors, Actuators and Microsystems, Barcelona, Spain, June 16 - 20, 2013, pp. 653-656.*

CONTACT

*L. Zhao, luruizha@usc.edu